

Oxidation Behavior of Molten Tin Doped with Phosphorus

AI-PING XIAN^{1,2} and GUO-LIANG GONG¹

1.—Shenyang National Laboratory for Materials Science, Institute of Metal Research, Chinese Academy of Science, 72 Wenhua Road, Shenyang 110016, P.R. China. 2.—e-mail: ap.xian@imr.ac.cn

The oxidation process of molten tin in air at 280°C was studied. We found that a trace addition of phosphorus to the tin reduced the surface oxidation greatly by forming a protective film. The total thickness of the oxide film formed on the molten Sn-0.007wt.%P alloy was about 36 nm, which was composed of a layer of 6 nm SnO₂, 10–15 nm (Sn, P)O, and a transition layer. This oxide film was approximately a quarter of the thickness that formed on pure tin. The oxidized surfaces of different tin alloys were studied by scanning electronic microscopy (SEM) and X-ray photoelectron spectroscopy (XPS). Much higher segregation of phosphorus was observed on the subsurface of the oxide film, and the concentration of phosphorus in the oxide film was about 500 times greater than that of the bulk concentration. Based on this result, the segregation of phosphorus on the molten surface could result in the formation of a new protective (Sn, P)O film on the subsurface of the molten tin. It is also suggested that the crystal structure of the oxide film should be studied in the future to confirm the mechanism.

Key words: Sn, oxidation, liquid, soldering, phosphorus

INTRODUCTION

The oxidation of molten solders composed of tin-based alloys in air is a severe problem in lead-free wave soldering. Dross, a mixture of molten tin and its oxide,¹ forms on the surface of molten solders and can cause many problems in the wave soldering process. For example, the formation of the dross may result in a heavy loss of the molten solder, thereby increasing the cost of the solder. Another problem is that the dross may cause a deterioration of the wetting properties and solderability of the surface of the molten solder.² In order to keep a clean surface of the molten solder the dross must be periodically removed manually.

Since the density of lead-free solders (approximately the density of molten pure tin 6,980 kg/m³ at the melting point³) is approximately the same as that of the tin oxides (SnO₂ 7,010 kg/m³, SnO 6,450 kg/m³),⁴ it is difficult to separate the dross from the molten solder bath by flotation. By com-

parison, the density of tin-lead solder is 8,900 kg/m³ and the dross is easy to float out in this case.

Moreover, since tin is a dominant component in lead-free solders, where tin comprises more than 95% in the alloy (Sn-Ag, Sn-Cu, and Sn-Ag-Cu, which are considered to replace Sn-Pb alloys) and the melting point of the solders is about 30°C higher than that of tin-lead eutectic solder. A higher temperature will increase the oxidation of the molten solders. Furthermore, the oxidation behavior of the molten solders is dominated by the oxidation of pure tin,⁵ and higher tin concentration in lead-free solders also result in increased oxidation. Therefore, compared with tin-lead solder, the problems associated with the oxidation of the molten lead-free solder are more severe, and a lead-free solder with oxidation resistance would be useful in electronic package, especially for wave soldering.

The oxidation of molten tin begins even at a very low oxygen partial pressure.⁶ In order to decrease the oxidation of the molten tin, doping with a trace element in pure tin is carried out in this work, by which the doping element will segregate on the surface of the molten tin quickly. The surface

(Received May 24, 2007; accepted August 20, 2007; published online September 21, 2007)

segregation of the doping element phosphorus affected the oxidation resistance of the molten tin dramatically. The effect of trace phosphorus in molten pure tin on the oxidation was studied in this work and was found to be effective to decrease the oxidation of molten tin in air.

EXPERIMENTAL

Sample Preparation

The samples, each piece approximately 50 g, were prepared by melting in a resistance furnace in 600°C for 10 min. The raw materials were industry pure tin and a phosphorus-bearing intermediate tin alloy. The purity of the industry pure tin was more than 99.90 wt.%, with the main impurities in the pure tin being Pb (≤ 0.045 wt.%), Bi (≤ 0.015 wt.%), Sb (≤ 0.02 wt.%), As (≤ 0.01 wt.%), and Cu (≤ 0.008 wt.%). In order to achieve homogeneity each sample was melted twice in the same conditions. The content of phosphorus in each sample is listed in Table I, calculated from the adding amount of the phosphorus-bearing intermediate tin alloy. The industrial pure tin was used as a parallel blank sample to compare the oxidation resistance of the samples. A very thin layer of yellow coating was observed on the wall of the quartz tube after melting, which indicated that there was a small amount of volatilization of phosphorus during the melting process.

Oxidation Measurement

About 50 g of each sample was placed in a graphite crucible with a diameter of 28 mm and heated in a resistance furnace in air. The temperature of the molten alloy was held at $280^\circ\text{C} \pm 3^\circ\text{C}$, measured by a thin thermocouple dipped into the molten alloy. This temperature is slightly higher than practical soldering temperatures (typically about 260°C), since the melting point of pure tin is 232°C , which is 15°C higher than that of Sn-Ag-Cu solder. The surface of the molten alloy was directly observed during the experiment. After the alloy had melted and reached the required temperature, the initial oxide film on the surface of the molten alloy was carefully removed by hand with a stainless-steel tool, and a fresh metal surface with a silver color was observed. This fresh liquid metal surface was exposed to the air, as an initial clean condition, and then oxidation process started from this time.

In this experiment the color change of the surface film after oxidation of the molten alloy was observed visually with increasing oxidation time. The images of the oxide film were recorded by a digital camera

(Canon Power Shot A300). When a layer of the oxide film had formed the dross on the surface of the molten alloy was carefully removed manually, and the weight of the collected dross measured each time by an electronic balance (SHIMADZU AY120 with an accuracy of 0.1 mg). In the case of removing the dross by hand, there was a fluctuation of the data for the dross weight and the average data based on three tests is presented herein.

XPS Measurements

After exposure to air at 280°C for 1 h, the molten alloy and the graphite crucible were carefully removed from the furnace, and cooled rapidly in air to obtain a smooth surface. The solidification sample was sliced in sheets about 2 mm thick from the top surface of the ingot for X-ray photoelectron spectroscopy (XPS) measurements. Since the XPS measurement is sensitive to surface pollution, the samples must be prepared carefully to prevent contamination by hand contact.

The surface chemical analysis of the samples was performed using XPS (ESCALAB 250 Model). The vacuum of the analysis chamber of the XPS was held at 10^{-8} Pa by a Ti pump during measurement, the energy of the monochromatic X-ray was 1486.6 eV (Al K_{α}), and the energy resolution of the analyzer was 0.05 eV. The original surface of each sample was first analyzed by XPS, and then to measure the underlying chemical composition after a very thin layer of the material was removed from the surface by Ar^+ sputtering.

The surface sputtering of the oxide film was carried out by an Ar^+ sputtering gun attached to the XPS spectrometer. The sputtering rate S (in units of meters per second) can be estimated from the following equation:⁷

$$S = \frac{I \cdot Y \cdot M}{\rho \cdot N_A \cdot e}$$

where I = primary ion current density, 0.5 A/m^2 ; Y = sputter yield, 6.8 atoms/ion at 2 keV^8 (for tin); M = atomic mass number, 118.7 g/mol (for tin); ρ = density, $7.3 \times 10^3 \text{ kg/m}^3$ (for tin); $N_A = 6.02 \times 10^{23}$ per mole (Avogadro number); and $e = 1.6 \times 10^{-19} \text{ A s}$ (the electron charge).

Based on this relationship the sputtering rate of the pure tin was estimated as 0.6 nm/s. However, this is only an approximate estimation as the real sputtering rate is dependent on many factors. For example, in the above function the sputter yield should be measured by experiment. Moreover, the value of 0.6 nm/s is only for pure solid tin, but in the

Table I. The P Content in Different Samples Used in this Study (wt.%)

	Pure Sn	Sn-0.0042P	Sn-0.0056P	Sn-0.007P	Sn-0.014P
P	0	0.0042	0.0056	0.0070	0.0140

present work the top surface of the sample was composed of both tin oxide and metal tin. The sputter yield for metal tin and tin oxide are considerably different, but data for the sputter yield of tin oxide is not currently available. Based on this consideration, the sputtering depth shown in the present work is only a semiquantitative value, while the sputtering time is the real data.

After sputtering for 10–60 s each time the fresh surface was again measured by XPS. The pure tin sample was sputtered eight times, while the other samples were sputtered only five times since the thickness of the oxide film for pure tin is relatively high. The total thickness to be removed by Ar⁺ sputtering was between 70 nm and 150 nm for different samples. The operation of the sputtering and measurement was repeated until the oxygen content on the surface measured by XPS was close to zero.

The reported data of the binding energy has been calibrated by both the residual carbon adsorbed on the original surface of the samples and the Ar⁺ induced during sputtering, which was located at 284.6 eV for the carbon peak and 241.9 eV for the Ar peak. The XPS Peak-Fitting Programme version 4.1⁹ was applied for the analysis of the XPS patterns. The value of the reference binding energy for each element was taken from the reference database.¹⁰

RESULTS AND DISCUSSION

Observation of the Oxidation

The liquid industrial pure tin was easily oxidized in air. After removal of the original oxide film on the surface of the molten tin, the fresh surface remained silvery for only about 3 min at 280°C before a slightly yellow oxide film formed quickly on the molten surface. With continued exposure to air the oxide film on the surface of the molten tin presented a sequence of different colors, in order of observation: golden yellow, red brown, purple, and dark purple. All the color changes took place within 60 min, during which time a thick layer of oxide formed on the surface. After exposure at 280°C for 60 min the dross was removed from the surface of the molten tin. The oxidation process was continuously observed with the dross removed at 60 min intervals.

As a comparison, the oxidation behavior of molten tin doped with phosphorus is obviously different from that of pure tin. In the case of Sn-0.0042wt.%P, under the same oxidation conditions, the fresh liquid surface remained bright silver during the first 2 h. After removing the dross twice the oxidation resistance of the molten metal decreased rapidly, in this case after the fresh surface was exposed to air for only a few minutes an oxide film with a slightly yellow color formed.

The amount of dross formed on the surface of molten tin doped with phosphorus was less than

that formed on the pure tin sample. After removing the dross three times the surface color of the sample began to change in the sequence: slight yellow, yellow, and slight red brown. However, when kept at 280°C without removing the dross, the surface remained bright silver for several hours, and the liquid surface exhibited a slight roughness. It seemed that continuous removal of the dross reduced the oxidizing resistance of the liquid alloy. This phenomenon could be a result of phosphorus consumption in the micro-alloy due to dross removal because of phosphorus segregation in the dross. The other samples doped with phosphorus showed similar phenomenon during the oxidizing process. However, the bright silvery surface of other samples doped with phosphorus remained during the whole testing and no discoloration was observed.

Figure 1 shows the colors of the surfaces oxides after dross removal five times (at 60 min intervals) at 280°C in air. This clearly indicates that, when the concentration of the doping phosphorus was lower, there was a similar color (Fig. 1a and b) of the oxide film on the pure tin and Sn-0.0042wt.%P sample. As a comparison, when the concentration of the doping phosphorus was higher the bright silver color remained at the end of the experiment. This implies that frequent dross removal could result in increased phosphorus consumption.

We observed by eye that the surface of molten pure tin was relatively smooth during oxidation compared to the surface of the molten Sn-P alloy. The higher the phosphorus content in the molten alloy, the rougher the surface film appeared. The scanning electronic microscopy (SEM) images in Fig. 2 clearly show that the oxidation surface of Sn-0.0042wt.%P is rougher than that of the pure tin sample. The rough surface film on the molten Sn-P alloy showed that, in the case of doping phosphorus in tin, there is an increase of volume during oxidation, that is, the volume of the solid oxide film on the molten tin is more than that of the metal consumed, which would result in a full coverage of the surface of the molten tin. This is the prerequisite to form a protective oxide film to prevent further oxidation of a solid metal.¹¹ This prerequisite should also be true for a molten metal. However, information on the crystal structure of the oxidation film is not yet available. Measurement of the crystal structure of the oxide film on the molten alloy presents the main difficulty, as the film is too thin (sometime within 50 nm) to be measured by X-ray diffraction (XRD). In this case, it is suitable to use low-energy electron-loss spectroscopy (LEELS)⁶ or grazing-incidence X-ray diffraction (GIXRD)¹² to measure the crystal structure of the film *in situ*; however, all methods to measure the crystal structure require a smooth surface and work in high-vacuum conditions. How to measure the crystal structure of an oxide film formed on molten metal in air *in situ* is a challenging issue in the study of the oxidation behavior of a molten metal; it will be an interesting area in the future.

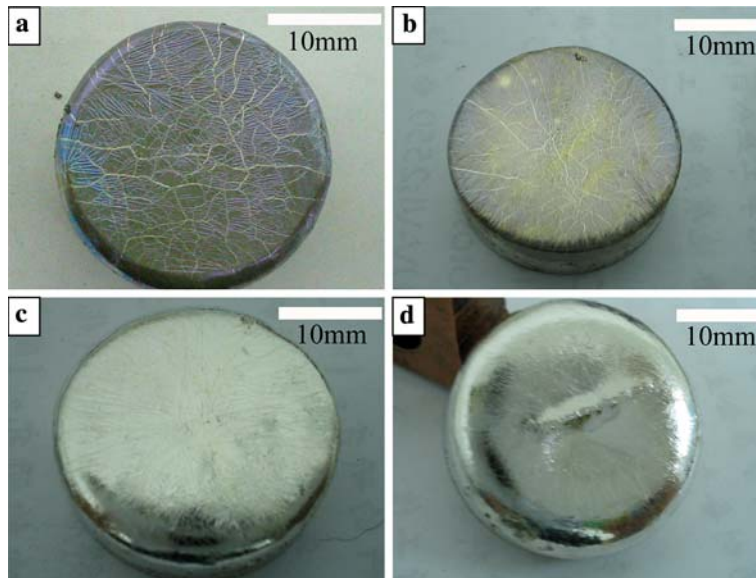


Fig. 1. The surface morphologies of the tin ingot after oxidized at 280°C for 60 min. in air (after removing the dross five times each with 60 min intervals): (a) pure tin, (b) Sn-0.0042wt.%P, (c) Sn-0.0056wt.%P, and (d) Sn-0.0070wt.%P.

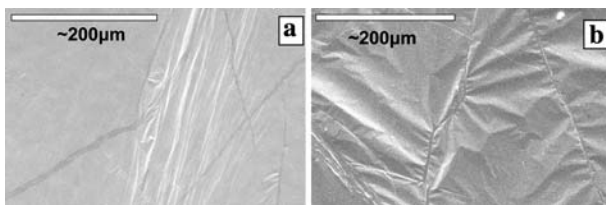


Fig. 2. SEM images of the oxidation surface after oxidized at 280°C for 60 min in atmosphere then rapidly cooling to room temperature: (a) pure tin (b) Sn-0.0042wt.%P.

Dross Weight

Figure 3 shows the relationship between the dross weight collected from the surface of different samples and the oxidation time. As mentioned in the Section “Observation of the Oxidation”, since the color of the films for different samples is different the curves of dross weight shown in Fig. 3 can only be regarded as a relative comparison of the different samples. Figure 3 does not imply real dynamic curves of the rate of the dross formation of an alloy at the experiment temperature.

As shown in Fig. 3 the rate of dross formation decreased dramatically for the phosphorus-doped samples. For all the samples the dross weight accumulated linearly with oxidation time. The slopes of the straight line shown in Fig. 3 are $4.7 \times 10^{-4} \text{ mg mm}^{-2} \text{ min}^{-1}$ for industry pure tin, $2.8 \times 10^{-4} \text{ mg mm}^{-2} \text{ min}^{-1}$ for Sn-0.0042wt.%P, $1.0 \times 10^{-4} \text{ mg mm}^{-2} \text{ min}^{-1}$ for Sn-0.0056wt.%P, $0.7 \times 10^{-4} \text{ mg mm}^{-2} \text{ min}^{-1}$ for Sn-0.007wt.%P, and $0.5 \times 10^{-4} \text{ mg mm}^{-2} \text{ min}^{-1}$ for Sn-0.014wt.%P. When the phosphorus concentration in the tin exceeded 0.0056 wt.%, the rate of dross formation was relatively slow, indicating the enhanced oxidation resistance of the molten alloy. In the case of

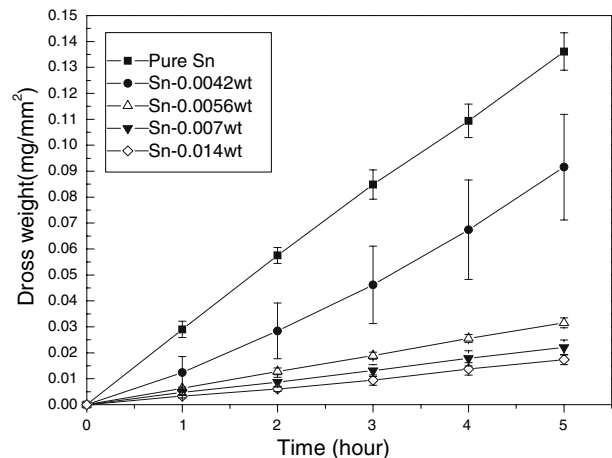


Fig. 3. The relationship between the accumulative dross weight on the surface and the oxidation time at 280°C (dross removal at 1 h intervals).

lower concentration of phosphorus (Sn-0.0042wt.%P) in the alloy, the fluctuation of the data of the accumulative dross weight is relatively significant. This fluctuation may be due to high surface segregation of phosphorus lost in the dross removal. Therefore, to increase the oxidation resistance of molten tin a critical phosphorus concentration in the alloy will be necessary.

XPS Analysis of the Oxidation Film

Pure Tin

Figure 4 shows the distribution of oxygen and tin along the depth direction of the oxide film. The total thickness of the oxide film of the pure tin sample after 60 min oxidation at 280°C was about 150 nm. The ratio of Sn and O on the surface was about 4:6,

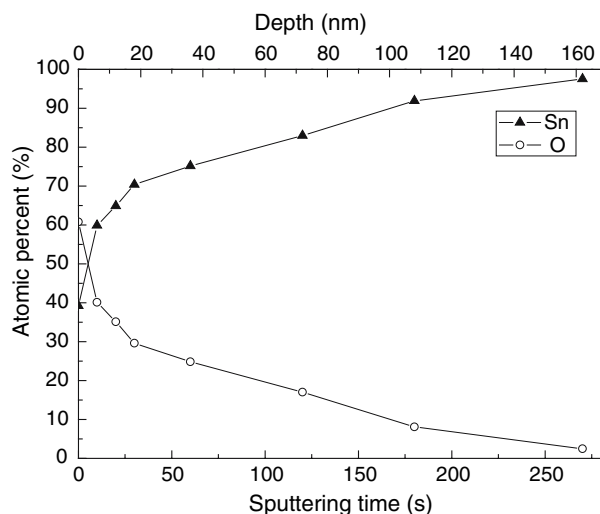


Fig. 4. The atomic percentage of Sn and O of the oxidation film measured by XPS after sputtering for various time for the pure tin sample oxidized at 280°C.

but rapidly increased to 6:4 after sputtering for 10 s with Ar^+ ions. It is difficult to determine the oxidation from these semiquantitative results alone since it should be considered that there will be both adsorption of oxygen on the surface and metallic tin atoms under the oxide film. However, based on the results shown in Fig. 5a, the oxygen adsorption on

the surface, if any, is relatively low. Assuming low surface oxygen adsorption, the ratio of oxygen to tin atoms measured by XPS should approach 1:1. The oxygen/tin ratio gradually decreased to about 3:7 within 20 nm from the surface.

Figure 5 shows the O_{1s} spectra of pure tin sample along the depth of the oxide film, in which the spectral factoring of both O chemically bound with tin and the adsorbed oxygen on the surface was present. The peak position of the O chemically bound with tin was located at 530.9 eV and the peak position of the adsorbed oxygen was located at 532.5 eV. It is obvious that the amount of adsorbed oxygen is much lower than that of the O chemically bound with tin. After the first sputtering for 10 s the adsorbed oxygen on the surface was entirely removed, producing the symmetrical and sharp peak pattern shown in Fig. 5b.

Figure 6 shows the XPS patterns of the Sn_{3d} peak of the pure tin sample at different depths in the oxide film. Based on the results in Fig. 6 there are two kinds of chemical states of tin: tin oxides and metallic tin, the latter being from the substrate. The peak position of the metallic tin, Sn^0 , is located at 484.8 eV, while the peak position of the tin oxides is located at 486.3 eV. As the difference of the peak position of Sn^{2+} and Sn^{4+} is very small these states cannot be distinguished from one other. With increasing depth, it is obvious that the proportion of tin oxide decreased and that the peak position of the

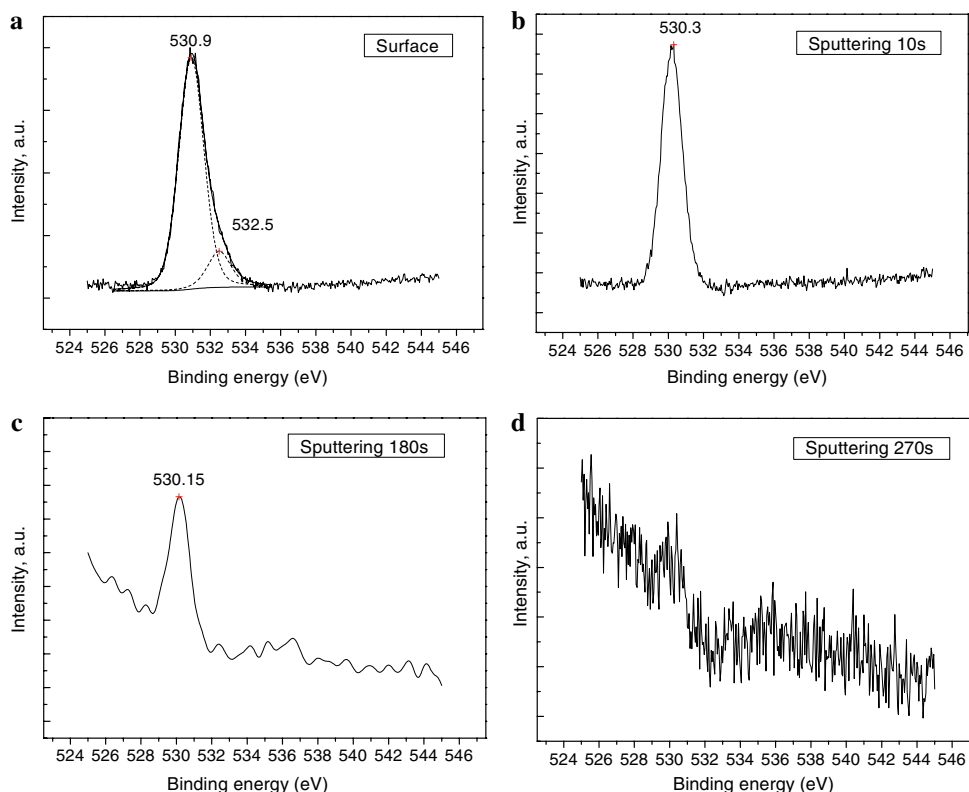


Fig. 5. A set of the O_{1s} spectral windows of the pure tin sample oxidized at 280°C for 60 min after sputtering for different time: (a) original surface, (b) sputtering 10 s, (c) sputtering 180 s, and (d) sputtering 270 s.

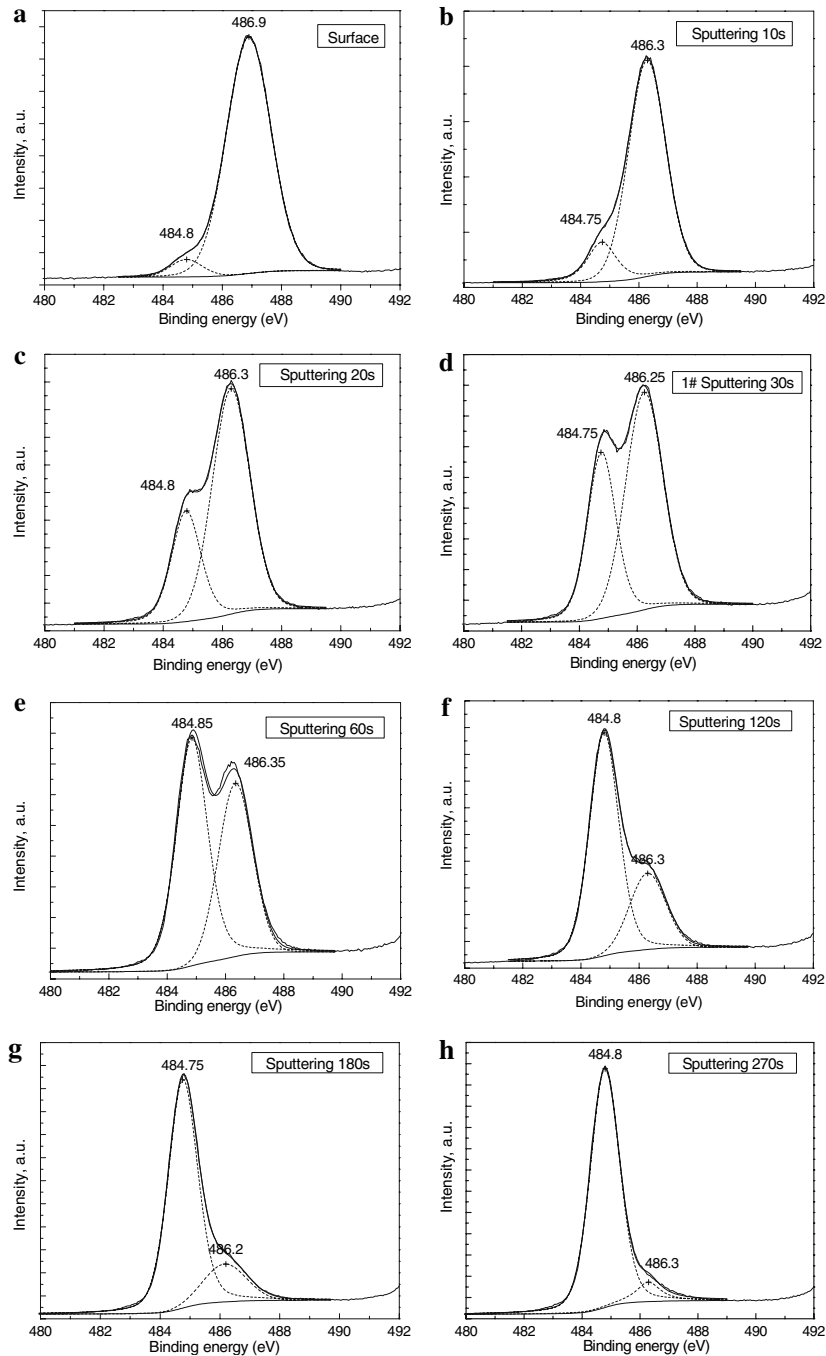


Fig. 6. XPS $\text{Sn}_{3d5/2}$ spectral window of the pure tin sample oxidized at 280°C for 60 min after sputtering for different time: (a) original surface, (b) sputtering 10 s, (c) sputtering 20 s, (d) sputtering 30 s (e) sputtering 60 s, (f) sputtering 120 s, (g) sputtering 180 s, and (h) sputtering 270 s.

$\text{Sn}_{3d5/2}$ spectrum gradually changed from 486.3 eV (tin oxides) to 484.8 eV (metallic tin). Figure 6 also shows the $\text{Sn}_{3d5/2}$ spectral factoring for the Sn^0 and the tin oxides. A semiquantitative analysis of the ratio of metallic tin to tin oxides is shown in Table II.

Table III shows data for the binding energy of SnO_2 , SnO , and metallic tin. Based on the results in Figs. 5 and 6, the Sn peak under the subsurface is located at 486 eV and the O peak is located at 530 eV. Both peaks are consistent with the SnO data shown in Table III.

Therefore, it is assumed that the outer surface of the oxide film of the pure tin sample should be SnO_2 with a little adsorbed oxygen and that the thickness of the SnO_2 is less than 6 nm. Under the SnO_2 there should be SnO film with a thickness of about 100 nm.

Sn-0.007wt.%P

Figure 7 shows the semiquantitative XPS results along the depth of the oxide film of the Sn-0.007wt.\%P sample. Three elements, Sn, P, and O, are measured on the surface of the oxide film.

Table II. The Relative Concentrations Sn^{2+} or $\text{Sn}^{4+}/\text{Sn}^0$ Measured by XPS for the $\text{Sn}_{3d5/2}$ Peak (pure tin sample oxidized in atmosphere at 280°C)

Sputtering time (s)	0	10	20	30	60	120	180	270
Peak position of Sn^0 (eV)	484.8	484.8	484.8	484.8	484.8	484.8	484.8	484.8
Peak position of Sn^{2+} or Sn^{4+} (eV)	486.9	486.3	486.3	486.3	486.4	486.3	486.2	486.3
Sn^{2+} or $\text{Sn}^{4+}/\text{Sn}^0$	18.69	6.05	2.40	1.60	0.75	0.39	0.22	0.03

Table III. Binding Energy Data for $\text{Sn}_{3d5/2}$ and O_{1s} from National Institute of Standards and Technology (NIST)¹⁰

Existing state	SnO_2	SnO	Sn^0
Binding energy of $\text{Sn}_{3d5/2}$ (eV)	487.1	486.0	484.8
Binding energy of O_{1s} (eV)	531.0	530.1	–

Similar to the result shown in Fig. 4 for pure tin, the outer surface of the oxide film was mainly composed of tin and oxygen, with very little phosphorus present. The atomic ratio between oxygen and tin on the surface of the oxide film was approximately 6:4. However, in contrast with the results for pure tin, there was a sharp chemical gradient along the depth of the Sn -0.007wt.%P oxide film. After a 10 s Ar^+ sputtering, during which a thickness of about 6 nm was removed, the phosphorus content increased to 8 at.%, while the tin content was 42 at.%, and the O content was about 50 at.%. The composition was relatively constant within a thickness of 6–12 nm, which implies there was a new phase of the oxide present. Based on the ratio of the composition this could be an Sn-P composite oxide, which could be assumed to be (Sn, P)O

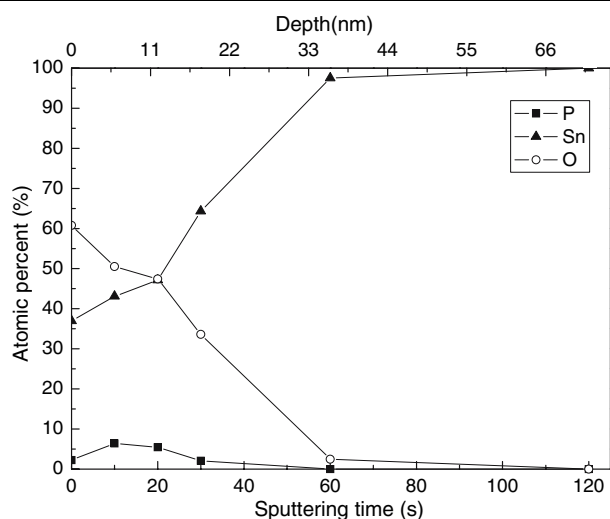


Fig. 7. The atomic percentage of Sn, P, and O of the oxidation film measured by XPS after sputtering for various times for the Sn -0.007wt.%P sample oxidized at 280°C.

in which phosphorus ions occupy about 20% of the position of tin ions. However, to the best of our knowledge this compound has not been reported previously.

Comparing the pure tin result shown in Fig. 4 and the Sn -0.007wt.%P result shown in Fig. 7, the total thickness of the oxide film of Sn -0.007wt.%P is about 36 nm, much thinner than that of pure tin. This shows that it is important to decrease the oxidation of molten tin by doping with trace phosphorus. The phosphorus content on the subsurface of the oxide film is up to 8 at.%, equal to about 4 wt.%, and phosphorus is highly segregated on the surface of the molten tin, where the concentration is more than 500 times than the bulk concentration. Figure 8 shows the XPS spectrum of the $\text{P}_{2p3/2}$ peak along the depth of the oxide film of the Sn -0.007wt.%P sample. The XPS peak height (estimated phosphorus content) on the subsurface of the oxidation is higher than on the outer surface. The detected segregation layer of phosphorus was very thin, distributed from a depth of about 6–12 nm from the outer surface. No phosphorus was detected by XPS below a depth of 36 nm from the outer surface. It is interesting that the peak position of $\text{P}_{2p3/2}$ in the oxide film is located at 133.4 eV, compared with peak positions (binding energy) of pure P and pyrophosphate of 130.2 eV and 133 eV, respectively, which implies that there is a new chemical state of P in the oxide. Based on Ref.¹³ this peak position for $\text{P}_{2p3/2}$ approaches that of pyrophosphate. However, further research is necessary to clarify the phosphorus mechanism in the protective oxide film.

Figure 9 shows the XPS result of $\text{Sn}_{3d5/2}$ along the depth of the oxide film of the Sn -0.007wt.%P sample. Similar to the results for pure tin shown in Fig. 6, the peak position of $\text{Sn}_{3d5/2}$ of the original outer surface was located at 487.15 eV. However, after removing 6 nm by sputtering, the peak position of $\text{Sn}_{3d5/2}$ was shifted slightly to 486.8 eV, after which it maintained its position until the tin oxide disappeared. It is not clear why both the binding energy of the outer surface and the subsurface were slightly greater than that of the pure tin oxide film. The binding energy of $\text{Sn}_{3d5/2}$ for the tetravalent tin ions Sn^{4+} is slightly higher than that for divalent tin ions Sn^{2+} .¹³ Combined with the result of the semi-quantitative analysis shown in Fig. 7, it is reasonable to assume that there is a double-layer oxide film structure. The outer surface should be SnO_2

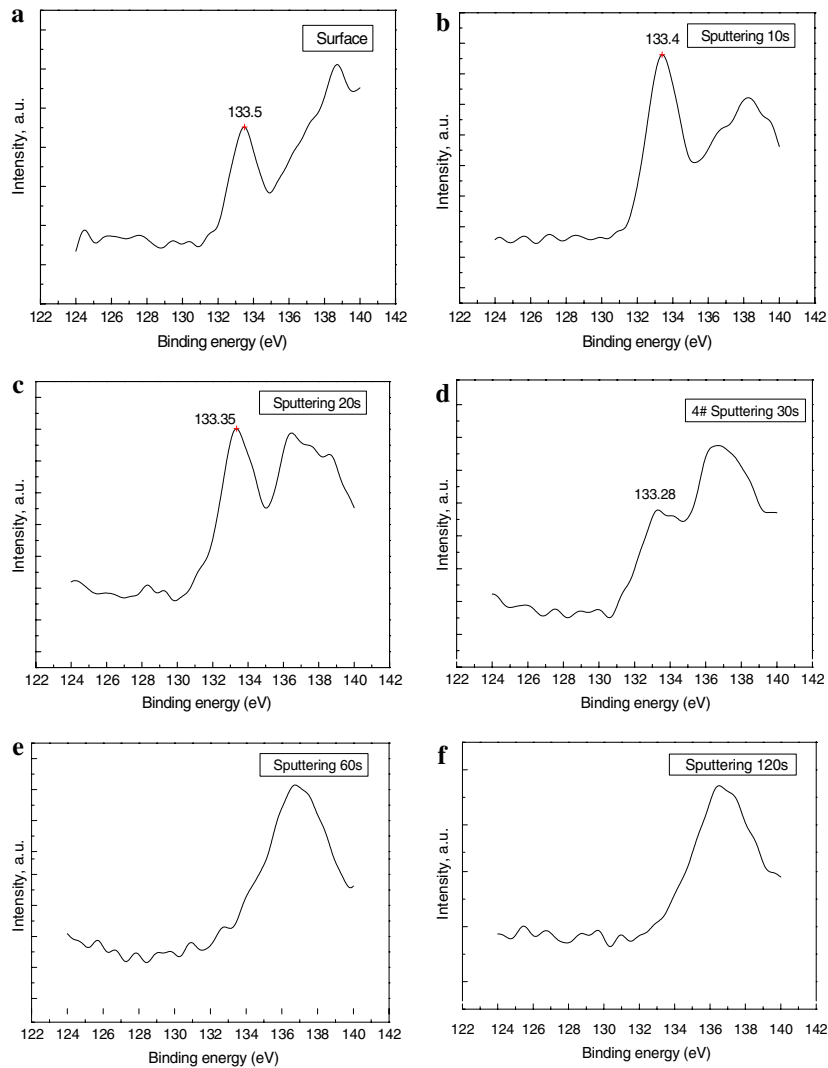


Fig. 8. $P_{2p_{3/2}}$ spectral windows of Sn-0.007wt.%P sample oxidized at 280°C for 60 min after sputtering for different time: (a) original surface, (b) sputtering 10 s, (c) sputtering 20 s, (d) sputtering 30 s, (e) sputtering 60 s, and (f) sputtering 120 s.

doped with phosphorus to a thickness of about 6 nm, and the subsurface should be an (Sn, P)O film with a thickness of about 10–15 nm, which could be a protective film to prevent further oxidation of the molten tin in air. The remaining thickness of the film should be a transition layer. After removing 36 nm from the surface by sputtering no oxide was detected by XPS. The peak position of metallic tin was located at 484.75 eV as shown in Fig. 9e and f.

Based on the XPS results, we propose that the oxide film for the Sn-0.007wt.%P sample can be considered as two layers. The outer surface is SnO_2 with a thickness of several nanometers. Due to direct contact with the air both C and O were adsorbed on the surface. On the other hand, the subsurface under the SnO_2 could be (Sn, P)O with a thickness of about 10–15 nm. This is a protective oxide film, by which the oxidation of the molten alloy is decreased dramatically.

CONCLUSIONS

The oxidation resistance of molten tin was greatly increased by doping with trace phosphorus. With the addition of 0.007 wt.% P, the surface of the molten tin can be kept silvery for several hours in air at 280°C.

A protective oxide film was observed by XPS on molten tin doped with phosphorus. The total thickness of the oxide film formed on the molten Sn-0.007wt.%P alloy was about 36 nm, composed of a layer of 6 nm of SnO_2 , 10–15 nm of (Sn, P)O, and a transition layer, in which the key protective film is (Sn, P)O. The composition of this film was measured by a semiquantitative XPS method, and contained 8 at.% P, 42 at.% Sn, and 50 at.% O. We propose that a new composite oxide film (Sn, P)O was formed. However, details of the protective film are not yet clear. It is suggested the crystal structure of the

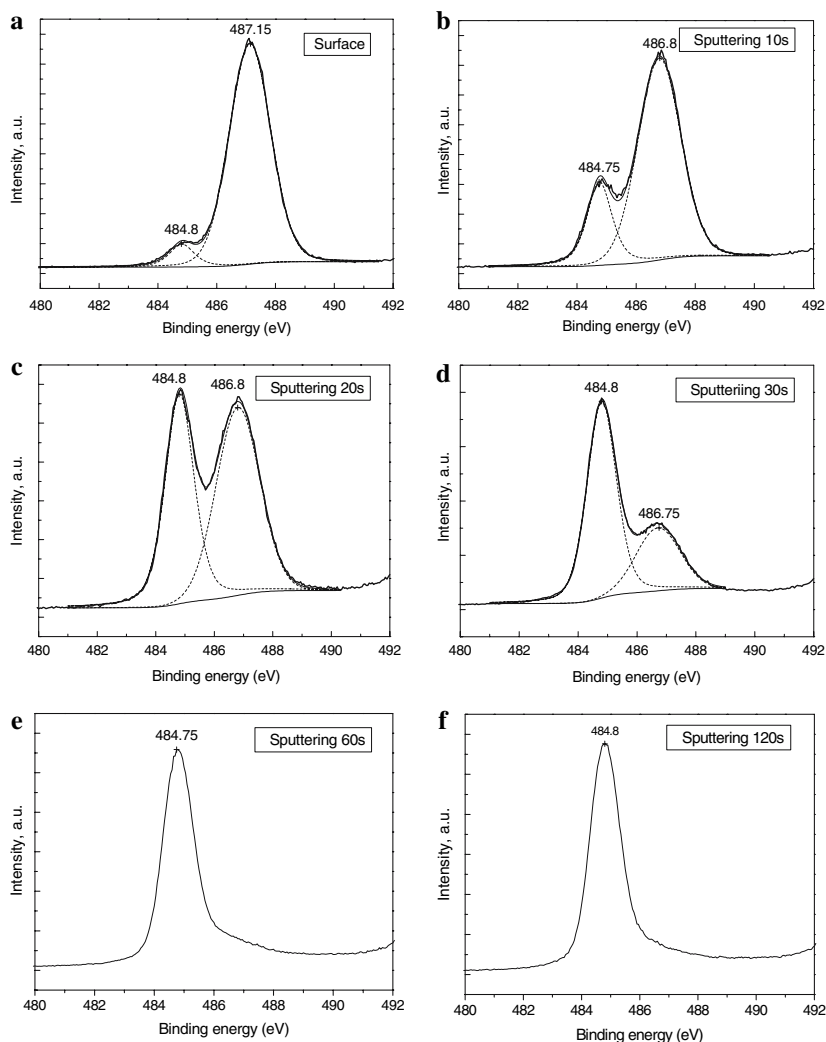


Fig. 9. XPS $\text{Sn}_{3d5/2}$ spectral windows of Sn-0.007wt.%P sample oxidized at 280°C for 60 min after sputtering for different times: (a) original surface, (b) sputtering 10 s, (c) sputtering 20 s, (d) sputtering 30 s, (e) sputtering 60 s, and (f) sputtering 120 s.

protective oxide film should be studied by LEELS or GIXRD in the future, while the *in situ* measurement of the crystal structure of a very thin oxide film formed on molten metal in air is a challenging issue in the study of the mechanism of oxidation behavior of a molten metal.

ACKNOWLEDGEMENTS

This research was supported by a High Technology Project of The Science and Technology Ministry of China (No. 2002AA322040), and the Shenyang Founding of Science and Technology in 2006. One of the authors thanks Prof. T. F. Li from the Institute of Metal Research at the Chinese Academy of Science for valuable discussion on the oxidation of metals, and the authors thank Dr. J. J. Guo and Mr. H. X. Zhao from the Institute of Metal Research at the Chinese Academy of Science for their assistance in preparing the experiments, and Mr. John Daghfal from the Institute of Metal Research at the Chinese Academy of Science and Mr. T. Rufford from the

University of Queensland for their help in improving the English of this paper.

REFERENCES

1. M. Arra, D. Shangguan, S. Yi, R. Thalhammer, and H. Fockenberger, *IEEE Trans. Electron. Packag. Manuf.* 25, 289 (2002).
2. G. Wable, Q.Y. Chu, P. Damodaran, and K. Srihari, *IEEE Trans. Electron. Packag. Manuf.* 29, 202 (2006).
3. T. Iida and R.I.L. Guthrie, *The Physical Properties of Liquid Metals* (New York: Oxford University Press, 1993), p. 71.
4. W.S. Huang, *Tin* (Beijing: Metallurgical Industry, 2000), p. 10 (in Chinese).
5. J.F. Kuhmann, K. Maly, and A. Preuss, *J. Electrochem. Soc.* 145, 2138 (1998).
6. A.J. Bevolo, J.D. Verhoeven, and M. Noack, *Surf. Sci.* 134, 499 (1983).
7. D. Briggs and M.P. Seah, *Practical Surface Analysis* (New York: Wiley, 1983), p. 146.
8. Z. Wang and D.Q. Yang, *Vac. Low. Temp.* 9, 51 (1990) (in Chinese).
9. R.W.M. Kwok, XPS Peak Fitting Programme for WIN95/98 XPSPEAK Version 4.1, Department of Chinese, University of Hong Kong.
10. <http://www.srdata.nist.gov/XPS/>

11. J.M. Xiao and C.N. Cao, *Principle of Materials Corrosion* (Beijing: Chemical Industry, 2002), p. 91 (in Chinese).
12. M.J. Regan, H. Tostmann, P.S. Pershan, O.M. Magnussen, E. Dimasi, B.M. Ocko, and M. Deutsch, *Phys. Rev.* B55, 10786 (1997).
13. J.F. Moulder, W.F. Stickle, P.E. Sobol, K.D. Bomben, *Handbook of X-ray Photoelectron Spectroscopy*, ed. J. Chastain (Eden Prairie: Perkin-Elmer Corp., 1992).